Temporal Inhomogeneities in High-Resolution Gridded Precipitation Products for the Southeastern United States

Jeremy E. Diem[1]

[1]Department of Geosciences, Georgia State University, Atlanta, GA, 30303, USA

Correspondence to: Jeremy E. Diem (jdiem@gsu.edu)

Abstract. High-resolution gridded precipitation products are widely used in hydroclimatic analyses, ~~although~~yet their ~~long-term~~temporal stability has not been ~~thoroughly~~comprehensively evaluated. This study ~~investigates~~assesses temporal inhomogeneities in ~~five widely used precipitations~~six datasets—Daymet, gridMET, nClimGrid, PRISM~~,~~ AN (All Networks), PRISM LT (Long Term), and TerraClimate—across the southeastern United States during 1980–2024. Annual precipitation totals ~~were~~ derived from ~~both~~ monthly and daily ~~data and~~ products were compared with a regional reference time series constructed from 120 U.S. Cooperative Observer Program (COOP) gauges. Residual-mass curves ~~and~~ were used to diagnose departures from temporal homogeneity, and split-sample Mann–Whitney *U* tests ~~were applied to identify temporal inhomogeneities, and trend~~identified statistically significant discontinuities. Trend magnitudes were estimated using the nonparametric Kendall–Theil robust line. Significant ~~inhomogeneities were detected in most datasets, with nearly 80% of discontinuities concentrated between 2002 and 2018. These shifts corresponded~~ discontinuities closely ~~to~~aligned with changes in gauge-network composition and documented data-processing procedures. Wetting shifts in Daymet and PRISM ~~exhibited wetting biases linked to the~~AN coincided with rapid expansion of the Community Collaborative Rain, Hail, and Snow (CoCoRaHS) network and ~~the concurrent decline of~~declining COOP ~~gauges, whereas~~ coverage. Drying biases in nClimGrid ~~showed~~and, to a ~~drying bias resulting from increased~~lesser extent, PRISM LT were associated with increasing reliance on Automated Surface Observing System tipping-bucket gauges, which are known to underestimate rainfall. ~~Step increases~~Abrupt step changes in TerraClimate and gridMET ~~totals reflected transitions~~corresponded to modifications in input ~~data~~datasets and reprocessing of precipitation forcing fields. ~~These~~The inhomogeneities produced disparate multi-decadal trends ranging from 19 to 48 mm dec^{-1} compared with a non-significant reference trend of 30 mm dec^{-1}. ~~Among all datasets and~~ Two product combinations ~~tested, the~~ Daymet–nClimGrid ~~pair was the only one without detectable~~and Daymet–nClimGrid–PRISM LT—showed no statistically significant discontinuities over 1980–2024 and ~~reproduced~~produced trends within 10% of the reference trend ~~most accurately. This combination provides a~~. These combinations provide homogeneous, temporally consistent ~~dataset~~datasets for multi-decadal precipitation analyses across the Southeast. Despite a significant but modest discontinuity, PRISM LT remains a viable individual product with appropriate homogenization, although continued declines in COOP coverage warrant caution. Overall, the results demonstrate that unrecognized inhomogeneities in gridded precipitation products can substantially bias ~~regional~~ trend assessments and underscore the need to evaluate and, when necessary, combine datasets to ensure temporal stability in long-term hydroclimatic studies.

1 Introduction

High-quality, multi-decadal precipitation data are essential for research and decision-making. Such records enable rigorous assessment of variability and long-term trends (New et al., 2001) and provide a robust foundation for model calibration and evaluation (Döll et al., 2016; Tango et al., 2025). Reliable long-term observations also underpin integrated and adaptive management of water resources, supporting sustainable planning for agriculture, ecosystems, and regional development (Yang et al., 2021; Ferencz et al., 2024;).

Spatial limitations remain a persistent challenge in precipitation measurement. Although gauge networks provide the foundation for precipitation observation, gauge distribution is often sparse and uneven (Kidd et al., 2017). These deficiencies are most pronounced in complex terrain and other data-sparse regions (Michelon et al., 2021).

To extend coverage beyond existing gauges, gridded precipitation products were developed. These datasets integrate gauge, satellite, and reanalysis information through interpolation or merging algorithms to generate spatially continuous precipitation estimates (Mankin et al., 2025). Gauge-informed products generally provide higher spatial accuracy than those derived solely from remote sensing or reanalysis (Zandler et al., 2019; Muche et al., 2020; de la Fraga et al., 2024; Mankin et al., 2025). However, the limited availability of gauges in complex terrain still constrains accuracy, and many products perform poorly in mountainous regions (Zandler et al., 2019; de la Fraga et al., 2024; Wang and Tian, 2025).

High-resolution gridded precipitation products are particularly well-suited to the needs of the hydrology community, which relies on them more than any other discipline. Gridded precipitation datasets provide the spatially distributed input data required to drive hydrologic models (Livneh et al., 2015; Newman et al., 2015; Shuai et al., 2022). Among many other applications, gridded precipitation products are also employed to quantify basin-scale water balances (Laiti et al., 2018) and to support hydrologic forecasting and management (Mankin et al., 2025).

Despite the widespread use of gridded precipitation products, especially within the hydrology community, the temporal stability of these datasets remains insufficiently evaluated. Apparent long-term trends can be distorted by inhomogeneities—systematic, non-climatic shifts in the statistical properties of a time series (Peterson et al., 1998). Only a handful of studies (e.g., Guentchev et al., 2010; Mizukami and Smith, 2012; McAfee et al., 2014; Ferguson and Mocko, 2017; Henn et al., 2018) have explicitly identified or investigated such inhomogeneities in gridded precipitation products. Accordingly, this study evaluates the temporal stability of multiple high-resolution precipitation datasets across a large, climatically uniform region during 1980–2024. The objectives are to (1) detect and characterize temporal inhomogeneities and the factors contributing to them, (2) quantify biases that influence multi-decadal trends, and (3) determine which individual products or product combinations exhibit the greatest temporal stability for regional trend analyses.

This study focuses on the southeastern United States (Fig. 1), encompassing Alabama, Florida, Georgia, Mississippi, North Carolina, South Carolina, and Tennessee, with a total area of approximately 882,000 km². The Southeast was selected because much of it has a humid subtropical climate—hot summers, mild winters, and high annual precipitation (Kunkel et al.,

Formatted: Indent: First line: 0.25"

2013; Labosier and Quiring, 2013)—and includes numerous long-term reference gauges from the U.S. Cooperative Observer Program (COOP), the nation's most consistent climate network (National Research Council, 1998).

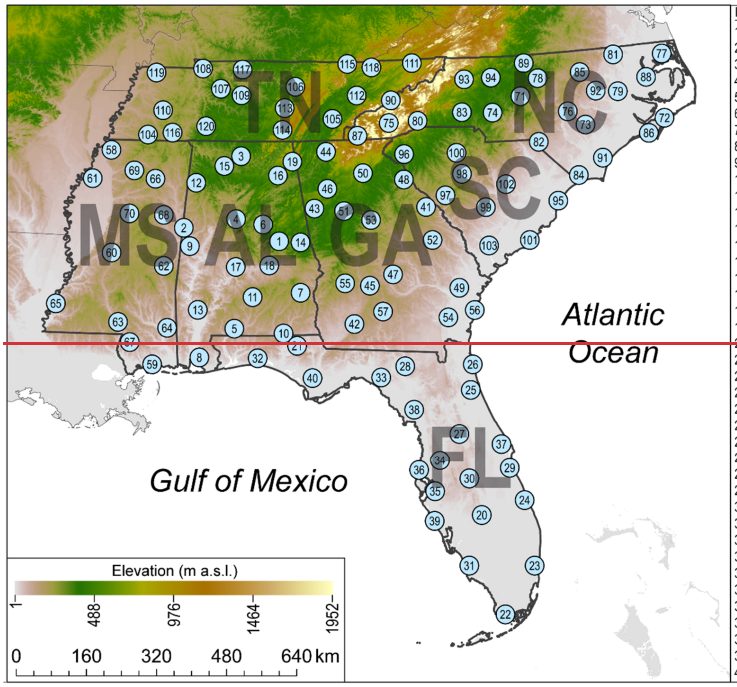

ID	COOP#	ID	COOP#	ID	COOP#
1	010160	41	090311	81	314456
2	010184	42	091500	82	314860
3	010655	43	091640	83	314996
4	010764	44	091863	84	315116
5	011080	45	092266	85	315123
6	011620	46	092485	86	315830
7	011725	47	092966	87	316001
8	012813	48	093060	88	316853
9	013160	49	093538	89	317202
10	013251	50	093621	90	319123
11	013519	51	094700	91	319467
12	013645	52	095863	92	319476
13	014193	53	095988	93	319555
14	014502	54	096219	94	319675
15	015635	55	097087	95	381093
16	017207	56	097808	96	381770
17	017366	57	098703	97	384607
18	018038	58	220237	98	385200
19	018469	59	220792	99	386527
~~20~~	~~088236~~	~~60~~	~~221389~~	~~100~~	~~387722~~
21	081544	61	221707	101	388405
22	083020	62	221860	102	388440
23	083163	63	221865	103	389469
24	083207	64	224966	104	400137
25	083874	65	226177	105	400284
26	084366	66	227106	106	402009
27	085076	67	227128	107	402489
28	085099	68	228374	108	402589
29	085612	69	229079	109	403280
30	085973	70	229743	110	404561
31	086078	71	310286	111	404858
32	086240	72	311606	112	404946
33	087025	73	311881	113	405882
34	087851	74	311975	114	406162
35	088782	75	312200	115	406493
36	088824	76	312500	116	408160
37	088942	77	312719	117	408562
38	089120	78	313555	118	408868
39	089176	79	313638	119	409219
40	089566	80	313976	120	409502

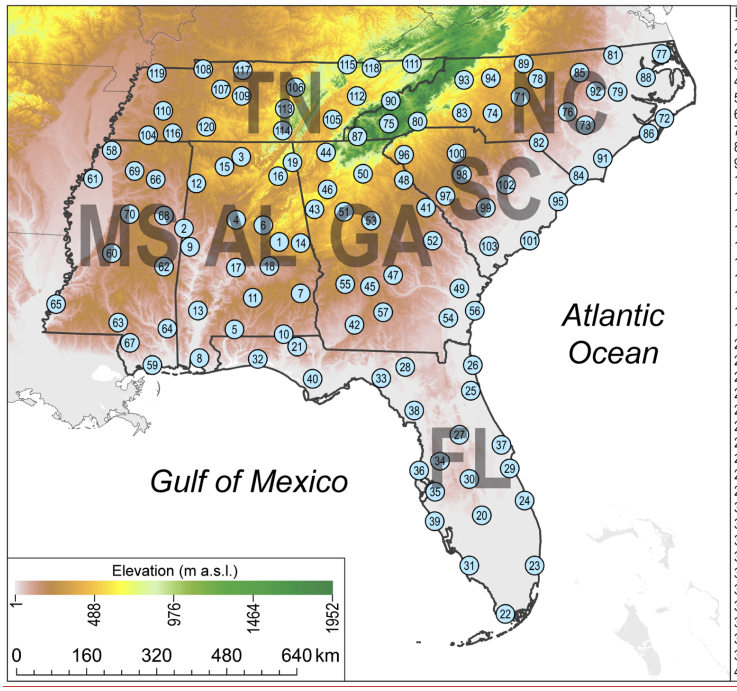

ID	COOP#	ID	COOP#	ID	COOP#
1	010160	41	090311	81	314456
2	010184	42	091500	82	314860
3	010655	43	091640	83	314996
4	010764	44	091863	84	315116
5	011080	45	092266	85	315123
6	011620	46	092485	86	315830
7	011725	47	092966	87	316001
8	012813	48	093060	88	316853
9	013160	49	093538	89	317202
10	013251	50	093621	90	319123
11	013519	51	094700	91	319467
12	013645	52	095863	92	319476
13	014193	53	095988	93	319555
14	014502	54	096219	94	319675
15	015635	55	097087	95	381093
16	017207	56	097808	96	381770
17	017366	57	098703	97	384607
18	018038	58	220237	98	385200
19	018469	59	220792	99	386527
20	080236	60	221389	100	387722
21	081544	61	221707	101	388405
22	083020	62	221860	102	388440
23	083163	63	221865	103	389469
24	083207	64	224966	104	400137
25	083874	65	226177	105	400284
26	084366	66	227106	106	402009
27	085076	67	227128	107	402489
28	085099	68	228374	108	402589
29	085612	69	229079	109	403280
30	085973	70	229743	110	404561
31	086078	71	310286	111	404858
32	086240	72	311606	112	404946
33	087025	73	311881	113	405882
34	087851	74	311975	114	406162
35	088782	75	312200	115	406493
36	088824	76	312500	116	408160
37	088942	77	312719	117	408562
38	089120	78	313555	118	408868
39	089176	79	313638	119	409219
40	089566	80	313976	120	409502

Figure ~~1.~~1. Locations of the 120 reference gauges in the southeastern United States. All gauges are part of the U.S. Cooperative ~~(USC) network.~~Observer Program (COOP). The seven states that comprise the southeastern United States are Alabama (AL), Florida (FL), Georgia (GA), Mississippi (MS), North Carolina (NC), South Carolina (SC), and Tennessee (TN).

2 Data

Monthly precipitation totals from a dispersed network of 120 COOP gauges across the Southeast during 1980-2024 were used to produce a reference time series (Fig. 1). All gauges had at least 90% of months with precipitation totals. Only 1.6% of gauge-months were missing. The missing monthly totals were replaced with the mean total from the three closest gauges. The gauges ranged in elevation from 1 m a.sl. to 668 m a.sl.; therefore, none of the gauges were located in high-elevation areas. Monthly totals for each gauge were summed to produce annual precipitation values, which were then averaged across all gauges to form the regional reference time series. Although COOP provides the longest regional record, documented observer-related biases indicate that non-climatic variability may persist (Daly et al., 2007).

Precipitation estimates were obtained for ~~five~~1980-2024 from the following high-resolution gridded products ~~(~~: Daymet, gridMET, nClimGrid, PRISM~~,~~ AN (All Networks), PRISM LT (Long Term), and TerraClimate~~) for 1980–2024. For each~~

product, annual precipitation totals were derived from the available daily and monthly data. Daymet provides daily precipitation estimates for North America at 1-km resolution, with monthly values derived by aggregating daily fields (Thornton et al., 2021). Daymet data were not yet released for 2024 at the time of analysis; therefore, the Daymet series extends through 2023. nClimGrid provides daily and monthly precipitation estimates for the conterminous United States at ~4-km resolution, generated independently using climatologically aided interpolation of station data (Vose et al., 2014). PRISM AN provides daily and monthly precipitation estimates for the United States at ~4 30 arc-second (~1 km nominal) spatial resolution, generated using station observations integrated with topographic and other spatial predictors (Daly et al., 2008). Because daily PRISM AN data were not available for 1980, annual totals for that year in the series were derived from monthly PRISM precipitation estimates to maintain a complete 1980–2024 record. PRISM LT data are similar to PRISM AN but are available only at monthly time steps and incorporate substantially fewer gauge networks than the AN product, a design choice intended to improve temporal stability for long-term analyses (Daly et al., 2021). gridMET provides daily precipitation estimates for the conterminous United States at ~4-km resolution, generated by combining high-resolution PRISM climatologies with temporally varying fields from the North American Land Data Assimilation System (NLDAS-2) using the METDATA downscaling method (Abatzoglou, 2013). TerraClimate provides monthly precipitation estimates for the global land surface at ~4-km resolution, generated by combining WorldClim climatologies with time-varying anomalies derived primarily from the Climatic Research Unit Time Series (CRU TS) and Japanese 55-year Reanalysis (JRA-55) datasets (Abatzoglou et al., 2018). When calculating regional means, which were compared with the mean of the 120 COOP gauges, approximately 2.5 % of grid cells (those exceeding 668 m a.s.l.) were excluded to restrict the analysis to the low- and mid-elevation portions of the Southeast and to minimize the aforementioned precipitation inaccuracies associated with mountainous areas.

Information on precipitation gauges underlying each gridded product was compiled for 1980–2024. Gauges were classified by network, and spatial coverage was assessed by identifying the 40-km grid cell containing each gauge across the Southeast. For each network, the number of grid cells containing at least one gauge was tallied and divided by the total number of grid cells in the region to calculate percent coverage.

In addition to analyzing each gridded product individually, time series were generated for all possible pairwise and multi-product combinations. Combinations were produced separately for the daily and monthly datasets, with each series calculated as the mean of the contributing products (e.g., Daymet and nClimGrid). For theAt each temporal scale, four products were available at both temporal scales, this yielded, yielding six two-product combinations, four three-product combinations, and one four-product combination, for a total of 11 unique combinations.

3 Methods

~~3.1~~3.1 Evaluating Spatial Agreement among Precipitation Products

To evaluate spatial agreement and quantify inter-product differences in annual precipitation totals, several complementary comparative analyses were conducted. All six precipitation products were resampled to a common 1-km spatial resolution to ensure direct cell-by-cell comparability across the southeastern United States. Cell-specific percent differences in mean annual precipitation totals over the 1980–2024 period (45-year mean) were calculated for all pairwise combinations of products (15 total comparisons). These calculations produced spatially explicit surfaces representing the magnitude and direction of inter-product differences. To quantify the overall level of agreement, the percentage of the 879,861 grid cells exhibiting absolute differences within ±5% was computed for each pairwise comparison.

3.2 Residual-Mass Curves

Residual-mass curves were constructed as a diagnostic of the homogeneity of precipitation time series and combinations of those series. This approach originates from hydrological consistency testing, in which cumulative residuals are plotted over time to reveal systematic deviations (Searcy and Hardison, 1960). In this study, residuals were obtained from linear regressions in which the reference time series served as the predictor and the product time series as the predictand. For a homogeneous record, the cumulative residuals are expected to remain near zero, fluctuating randomly without systematic drift, whereas sustained deviations or changes in slope indicate shifts, biases, or other inconsistencies (Buishand, 1984; Helsel and Hirsch, 2002).

3.~~2~~3 Testing for Differences

To identify the most significant discontinuity—defined here as an abrupt, non-climatic shift in a time series representing a temporal inhomogeneity—in each product time series, a nonparametric split-sample approach was applied. For each potential breakpoint year, residuals (i.e., observations minus product estimates) before and after that year were compared using the Mann–Whitney *U* test ($\alpha = 0.01$, two-tailed), with a minimum of eight years required in each group, yielding candidate breakpoints between 1988 and 2017. The Mann–Whitney *U* test has been shown to be effective for identifying shifts in hydroclimatic time series (Yue and Wang, 2002), and similar split-sample approaches have been applied in climate homogenization studies to test for differences before and after potential discontinuities (Easterling and Peterson, 1995).

3.~~3~~4 Trend Analyses

Trends in annual precipitation for 1980–2024 were computed for each gridded product and the reference time series. The Kendall–Theil robust line, calculated as the median of the slopes between all pairs of observations (Helsel and Hirsch, 2002), provided a nonparametric estimate of the trend magnitude. The statistical significance of each trend was assessed with Kendall's tau correlation test ($\alpha = 0.01$, one-tailed).

4 Results

4.1 Spatial ~~Variations in~~Agreement among Precipitation Products

Mean annual precipitation totals and spatial patterns ~~and totals are~~were broadly consistent among the ~~five~~six precipitation products, with Daymet producing slightly higher ~~values~~ totals and nClimGrid slightly lower totals than the others (~~Fig~~Figs. 2~~).~~ ~~This comparison provides spatial context for the subsequent temporal analyses by illustrating that the datasets yield similar climatological means across the Southeast.~~ and 3). Mean annual totals for 1980–~~2023 range~~2024 ranged from 1,~~347~~348 mm for nClimGrid to 1,~~431~~434 mm for Daymet~~. Precipitation~~, with precipitation totals ~~are~~ smallest (~1,100 mm) across central Georgia, South Carolina, and North Carolina and largest (~2,000 mm) in the Blue Ridge and Cumberland Mountains~~.~~ (Fig. 2). Inter-product differences in mean annual totals were remarkably small: among the 15 pairwise combinations, 67% to 98% of grid cells differed by no more than ±5%, with a mean of 89% of cells meeting this threshold (Fig. 3). The largest discrepancies were concentrated in the Appalachian and Cumberland Mountains and in southeastern Florida, although differences exceeding 15% were rare even in these areas. On average, Daymet produced totals 4.7% higher on average than the other products, whereas nClimGrid produced totals 2.3% lower on average, indicating modest wet and dry biases relative to the other products.

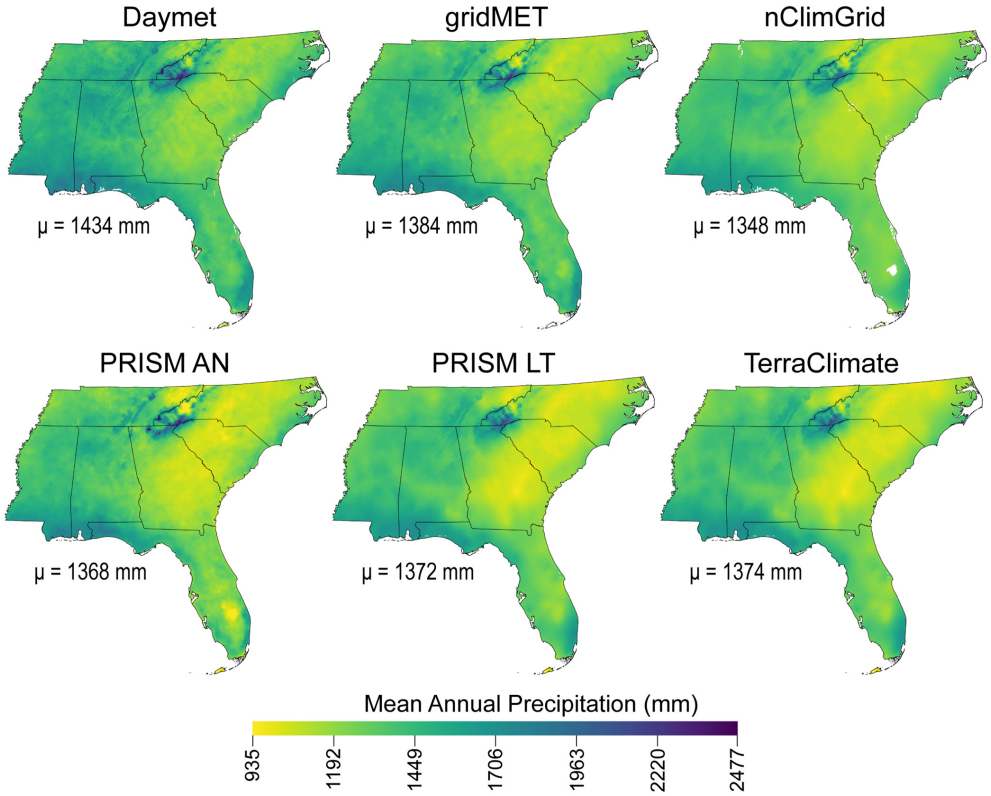

Figure 2. Mean annual precipitation totals (in mm) during 1980-2024 for the six precipitation products. gridMET, nClimGrid, PRISM AN, PRISM LT, and TerraClimate have been resampled to 1-km resolution to match the resolution of Daymet.

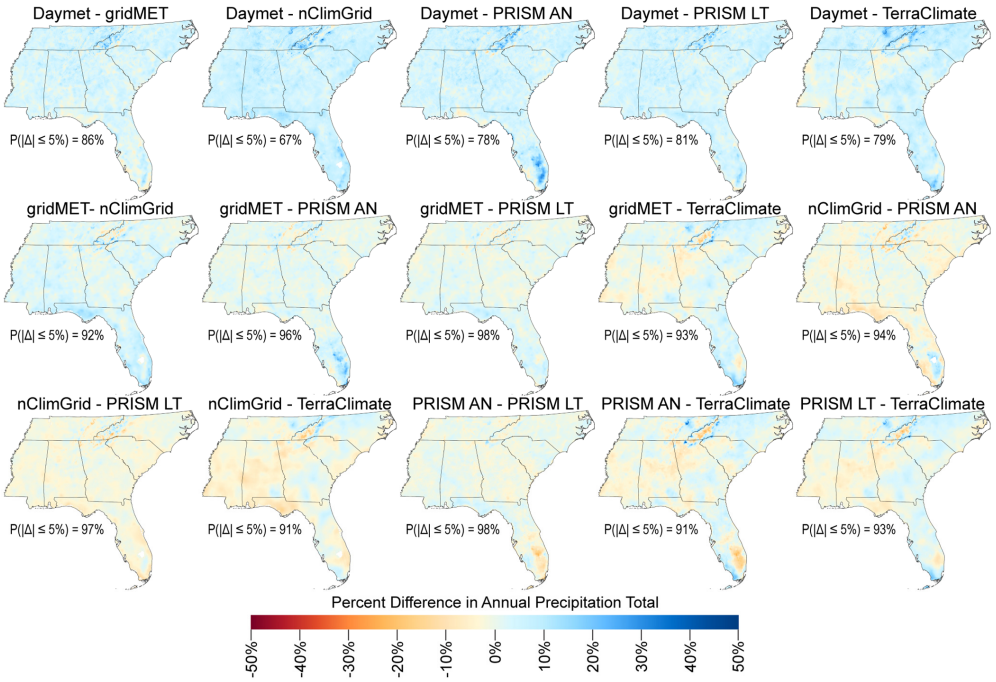

Figure 3. Percent difference in mean annual precipitation totals (1980-2024) between pairs of products. P(|Δ| ≤ 5%) is the percentage of grid cells with percent differences between −5% and 5%.

4.2 Changes in Gauges

All products showed substantial temporal changes in gauge numbers across 1980–2024, most notably increasing coverage by CoCoRaHS (Community Collaborative Rain, Hail, and Snow Network) gauges and decreasing coverage by COOP gauges (Fig. ~~3~~4). Daymet was initially dominated by COOP gauges but by the end of the period CoCoRaHS gauges were most prevalent. Both CoCoRaHS and ~~weather bureau~~first-order airport surface observing stations (hereafter, first-order gauges)

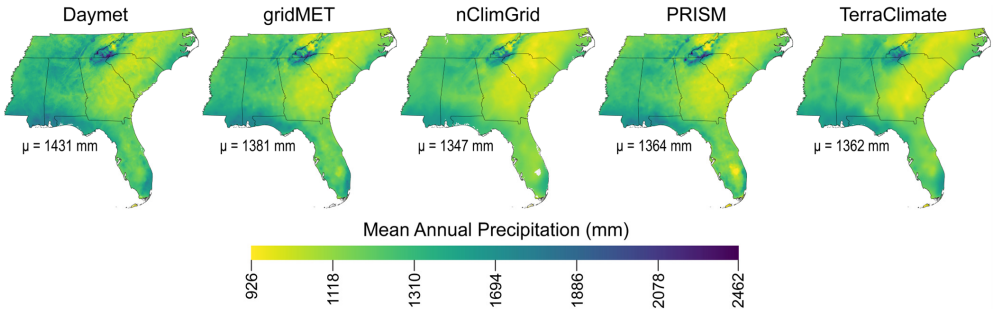

~~**Figure 2.** Mean annual precipitation totals (in mm) during 1980-2023 for the five precipitation products. gridMET, nClimGrid, PRISM, and TerraClimate have been resampled to 1-km resolution to match the resolution of Daymet.~~

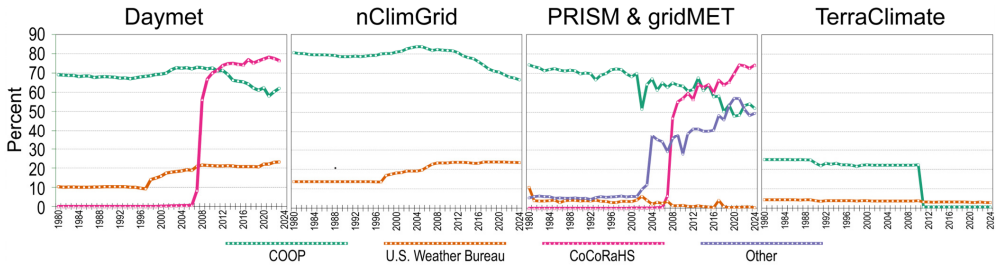

~~**Figure 3.** Differences in annual precipitation between monthly products and daily products.~~

increased in coverage, with CoCoRaHS rising from <1% in 2006 to 78% in 2021, while COOP gauges began decreasing around 2011. nClimGrid consistently relied more on COOP than ~~weather bureau~~first-order gauges, but the difference in 2024 (67% vs. 24%) was much smaller than in 1980 (81% vs. 14%). Coverage by ~~weather bureau~~first-order gauges began increasing in 1998, while COOP coverage declined after 2012. PRISM AN and gridMET, which used gauges from 15 networks, showed a similar pattern, with increasing CoCoRaHS and decreasing COOP coverage. CoCoRaHS coverage rose from <1% in 2006 to ~75% in 2021. There was also an increase in gauges from other networks and a steady decline in COOP coverage. PRISM LT was dominated by COOP gauges throughout the period, with COOP comprising between 48% and 74% of all gauges, while first-order gauges accounted for ~4% of coverage from 1980 to the early 2000s, after which RAWS coverage increased to ~8% by 2024. TerraClimate had much less gauge coverage overall, with a maximum of 25% from cooperative gauges and an abrupt decline from 22% to <1% between 2010 and 2011. ~~Information on gauge coverage for gridMET was unavailable.~~

~~4.3 Comparison of Monthly and Daily Versions of Products~~

~~Monthly and daily versions of Daymet, nClimGrid, and PRISM had either identical or nearly identical results (Fig. 4). Consequently, monthly results – which include TerraClimate – are shown in the paper, while the daily results – which include gridMET – are presented in the supporting information.~~

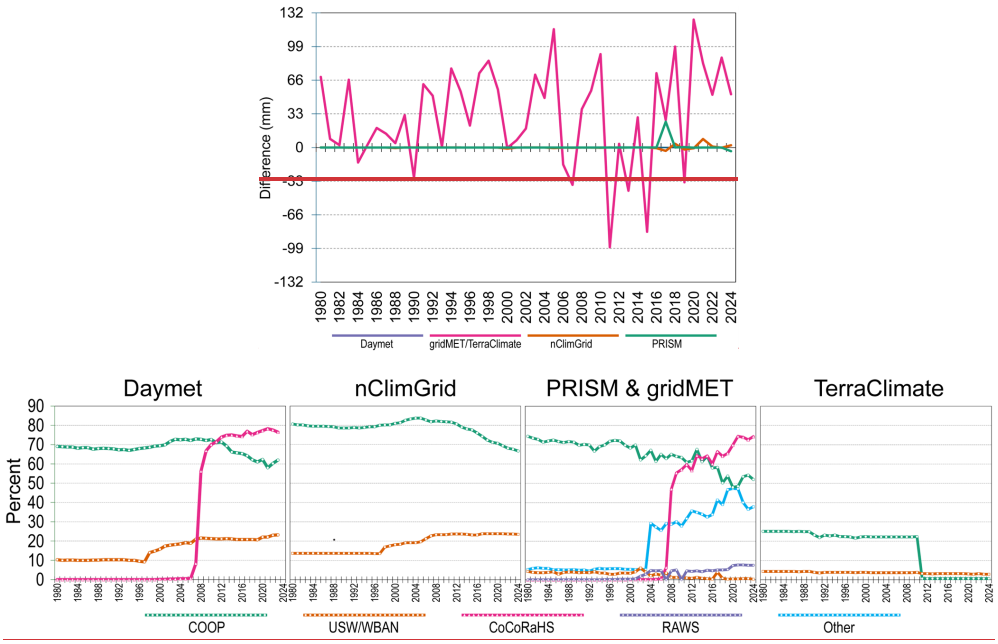

Figure 4. Percent coverage of the southeastern United States over time by gauge networks used in the ~~five precipitation products~~precipitation products. COOP is the U.S. Cooperative Observer Program. USW/WBAN gauges are first-order airport surface observing stations. CoCoRaHS is the Community Collaborative Rain, Hail and Snow network. RAWS is the Remote Automated Weather Stations network. With respect to the PRISM and gridMET panel, only COOP, RAWS, and first-order airport (WBAN) gauges are used to develop the PRISM LT product.

Formatted: Justified

Formatted: Font: 10 pt

4.3 Comparison of Monthly and Daily Versions of Products

Comparisons of monthly and daily product versions revealed consistent behaviour for some datasets but notable temporal differences for others (Fig. 5). Monthly and daily versions of Daymet and nClimGrid produced either identical or nearly identical results. In contrast, PRISM AN and PRISM LT exhibited distinct temporal behaviour and are therefore treated

separately in subsequent analyses. Consequently, monthly results—which include TerraClimate and PRISM LT—are shown in the paper, while the daily results—which include gridMET and PRISM AN—are presented in the supporting information.

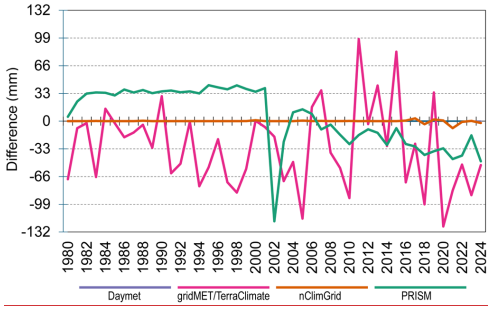

Figure 5. Differences in annual precipitation between monthly and daily products, 1980–2024.

4.4 Residual-Mass Curves

~~Among the initial~~ Combinations of products~~, Daymet had~~ produced the most optimal residual-mass ~~curve, and combining products resulted in the best residual-mass~~ curves ~~(~~Fig. ~~5~~overall, while performance among individual products varied substantially (Figs. 6 and S1). ~~The best residual-mass~~Optimal curves ~~are those with~~were characterized by relatively small cumulative sums of the absolute ~~values of~~ residuals. ~~Daymet had much lower~~Among the individual products, PRISM LT exhibited the lowest cumulative residual total, whereas PRISM AN exhibited the highest total. The lowest cumulative sums ~~than the other four initial products. The~~ overall ~~best products~~ were achieved by several multi-product combinations ~~of products, and those products were~~ , including (in ascending order) nClimGrid–PRISM, Daymet–nClimGrid–TerraClimate, Daymet–nClimGrid–PRISM, Daymet–gridMET~~–nClimgrid~~–nClimGrid, Daymet–nClimGrid, Daymet–nClimGrid–PRISM AN, and Daymet–nClimGrid–PRISM LT.

The residual-mass curves also revealed potential discontinuities, ~~most of~~ which occurred ~~during~~between the ~~third~~early 1990s and ~~fourth decades of the 45-year record~~2016 (Fig. ~~3~~6 and ~~S2~~S1). In each panel of the figures, the year associated with the largest absolute residual corresponded to the year preceding the potential discontinuity. For Daymet, gridMET, nClimGrid, PRISM AN, PRISM LT, and TerraClimate, the potential discontinuities were centered on ~~2008~~2012, 2016, 2005, 2002, 1999, and 2011, respectively. ~~For~~Across all products and product combinations ~~of products, over 80~~, 50% of the potential discontinuities occurred ~~during 2002~~ in 1993 and 2016 combined.

4.5 Discontinuities

Most products exhibited significant discontinuities, and the timing of these shifts generally aligned with the potential discontinuities identified from the residual-mass curves (~~Fig. 6~~Figs. 7 and S2). ~~Approximately 80 % of~~All but three products showed at least one significant discontinuity. The ~~initial~~individual products—Daymet, gridMET, nClimGrid, PRISM AN,

PRISM LT, and TerraClimate—had discontinuities centered on 2012, 2016, 2005, 2002, 1993, and 2011, respectively. ~~Nearly 90 % of all~~ Collectively, discontinuities~~, including those from product combinations, occurred between~~ across all products clustered within five periods: 1991–1993, 2002, 2005, 2011–2012, and ~~2018. A few products showed discontinuities in the early 1990s, all of which included nClimGrid as a component. Ideally, no discontinuities should be present in homogeneous time series, and the~~2016. The only products without detectable discontinuities were ~~TerraClimate,~~ Daymet–nClimGrid, Daymet–nClimGrid–PRISM LT, and nClimGrid–PRISM~~, and nClimGrid–PRISM–TerraClimate~~ AN.

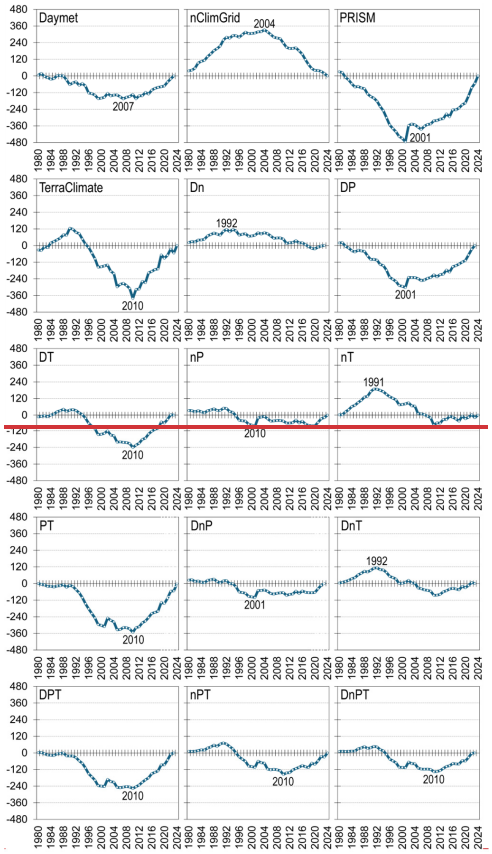

~~**Figure 5.** Residual-mass curves for products and combination of products. Abbreviations for Daymet, nClimGrid, PRISM, and TerraClimate, are D, n, P, and T, respectively.~~

4.6 Time Series of Differences

With respect to differences from the reference time series before and after a discontinuity, most products shifted from either ~~underestimates to overestimates or from~~ overestimates to larger overestimates, underestimates to larger underestimates, or underestimates to overestimates (~~Fig. 7~~Figs. 8 and S3). Daymet shifted from overestimates to larger overestimates. Both gridMET and PRISM AN shifted from underestimates to overestimates. ~~Daymet shifted from overestimates to larger overestimates.~~ nClimGrid shifted from underestimates to larger underestimates. PRISM LT and TerraClimate ~~did not exhibit a significant discontinuity and therefore showed no shift. Considering~~were relatively unique among all the products ~~collectively, about half~~, since PRISM LT shifted from overestimates to underestimates and TerraClimate shifted from underestimates to ~~overestimates, one-third from overestimates to larger overestimates, and roughly 17 % from underestimates to larger underestimates; none shifted from overestimates to underestimates.~~smaller underestimates.

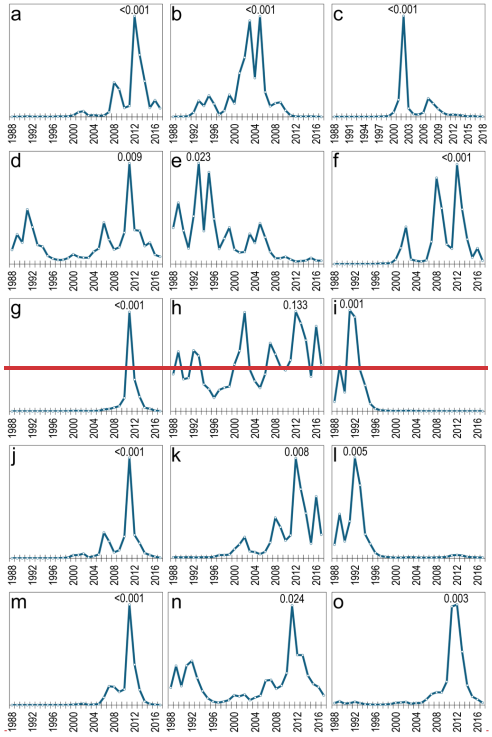
a
<0.001
b
<0.001
c
<0.001
d
0.009
e
0.023
f
<0.001
g
<0.001
h
0.133
i
0.001
j
<0.001
k
0.008
l
0.005
m
<0.001
n
0.024
o
0.003

234

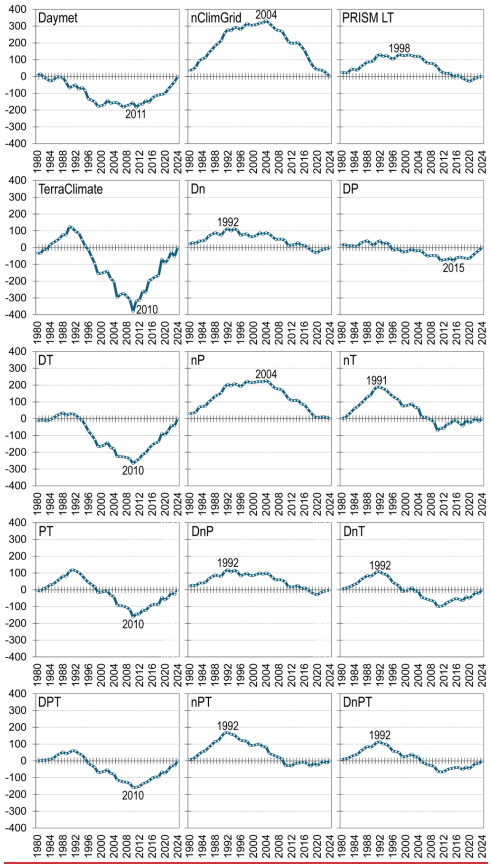

Figure 6. Residual-mass curves for products and combination of products. Abbreviations for Daymet, nClimGrid, PRISM LT, and TerraClimate, are D, n, P, and T, respectively. Units are mm.

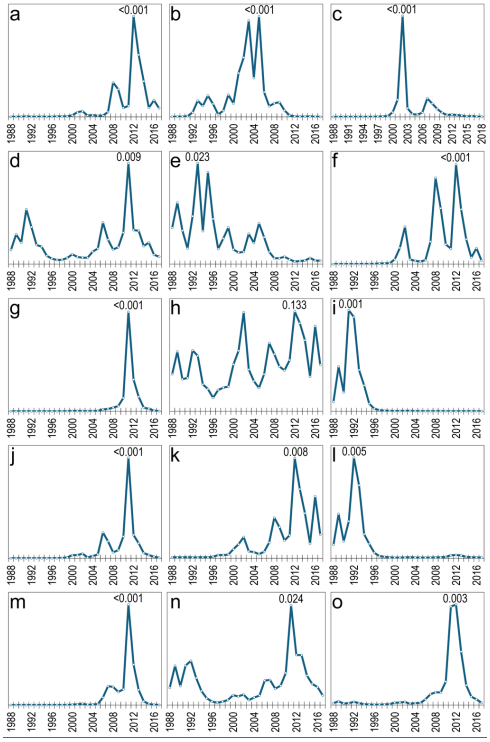

Figure 7. Inverse p-values for (a) Daymet, (b) nClimGrid, (c) PRISM LT, (d) TerraClimate, (e) Dn, (f) DP, (g) DT, (h) nP, (i) nT, (j) PT, (k) DnP, (l) DnT, (m) DPT, (n) nPT, and (o) DnPT. Abbreviations for Daymet, nClimGrid, PRISM LT, and TerraClimate, are D, n, P, and T, respectively. The two-tailed p-values are from Mann-Whitney *U* tests that compared differences from the reference time series before and after each of the years shown (i.e., 1988-~~2018).~~2017).

Formatted: Font: Not Italic

~~**4.7 Trends**~~

~~The products exhibited a wide range of precipitation trends, with only a few approximating the reference trend of 30 mm dec^{-1}, which was not significant (Fig. 8 and S4). Daymet, gridMET, nClimGrid, PRISM, and TerraClimate had trends of 38, 38, 19, 48, and 36 mm dec^{-1}, respectively. Among the individual products, nClimGrid produced the smallest trend and PRISM the largest trend. The trend for PRISM, as well as those for the combinations Daymet PRISM, Daymet gridMET PRISM, Daymet PRISM TerraClimate, gridMET PRISM, and PRISM TerraClimate, were statistically significant. The products within 10 % of the reference trend were Daymet gridMET nClimGrid, Daymet nClimGrid, gridMET nClimGrid PRISM, and nClimGrid TerraClimate.~~

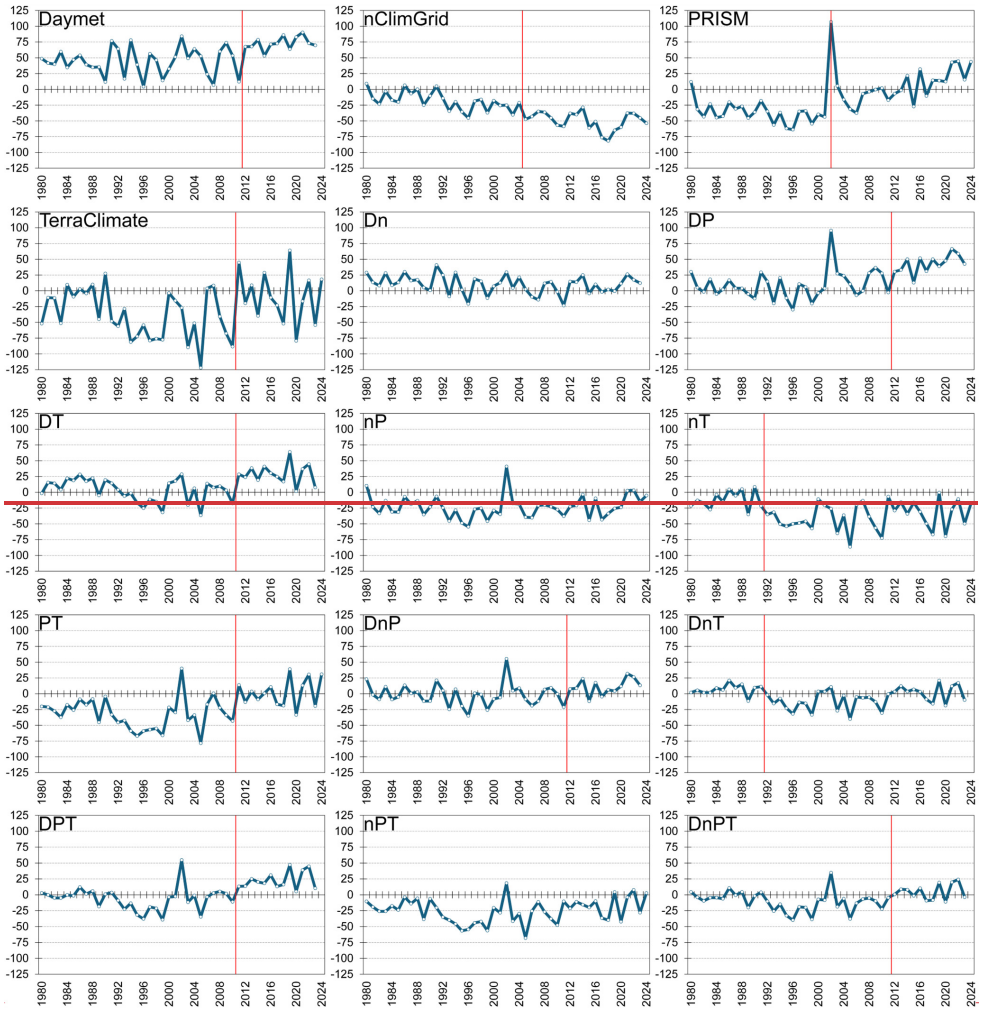
Daymet
nClimGrid
PRISM
TerraClimate
Dn
DP
DT
nP
nT
PT
DnP
DnT
DPT
nPT
DnPT

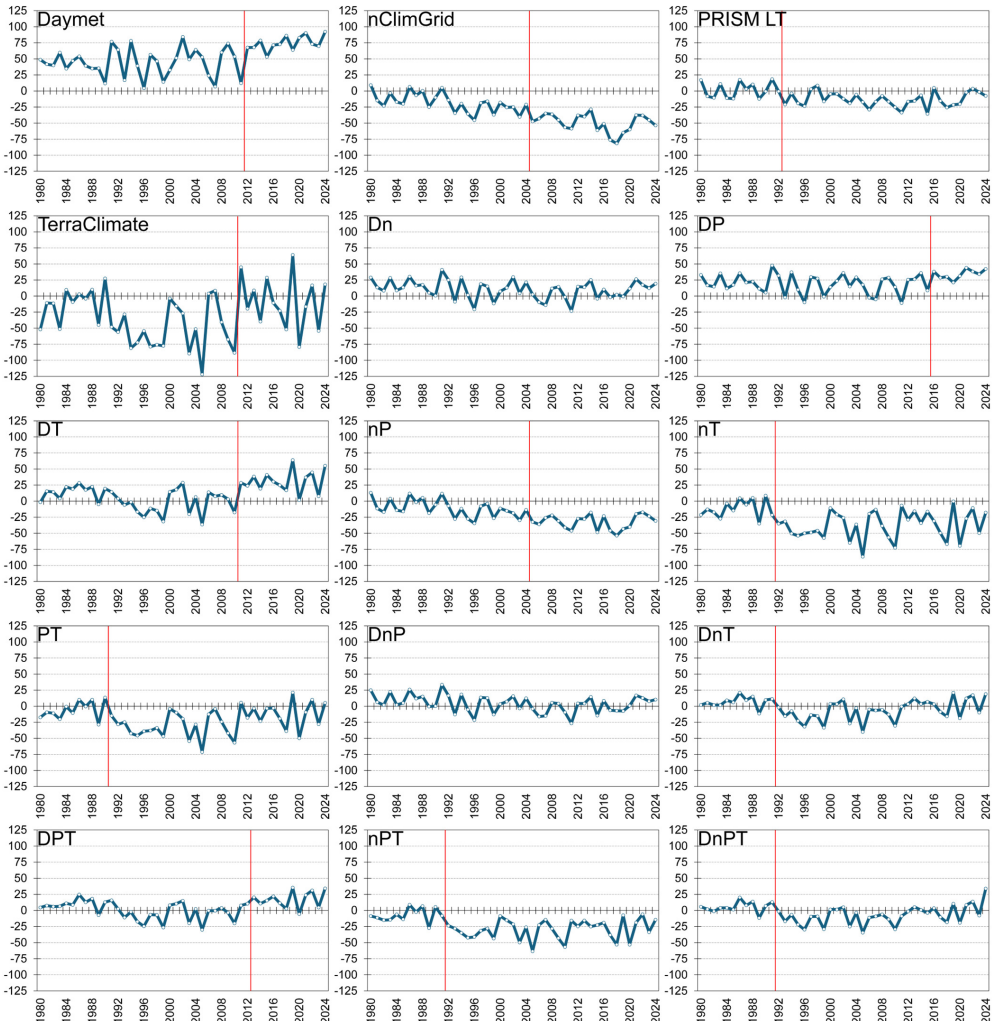

Figure 78. Time series of differences (in mm) between the mean of the 120 references gauges and the means for the southeastern United States that area specific to products and combination of products. Abbreviations for Daymet, nClimGrid, PRISM LT, and TerraClimate, are D, n, P, and T, respectively.

Formatted: Left

4.7 Trends

The products exhibited a wide range of precipitation trends, with only a few approximating the reference trend of 30 mm dec^{-1}, which was not statistically significant (Figs. 9 and S4). For the individual products, Daymet, gridMET, nClimGrid, PRISM AN, PRISM LT, and TerraClimate had trends of 39, 39, 19, 48, 27, and 37 mm dec^{-1}, respectively. Among all products, trends ranged from 19 mm dec^{-1} (nClimGrid) to 48 mm dec^{-1} (PRISM AN), with PRISM AN being the only product with a statistically significant trend. Products within 10% of the reference trend, listed in ascending order of deviation (with the first product closest to the reference), were Daymet–nClimGrid–PRISM LT–TerraClimate, Daymet–nClimGrid, PRISM LT–TerraClimate, gridMET–nClimGrid, Daymet–nClimGrid–PRISM LT, Daymet–nClimGrid–TerraClimate, nClimGrid–TerraClimate, nClimGrid–PRISM–TerraClimate, and PRISM LT.

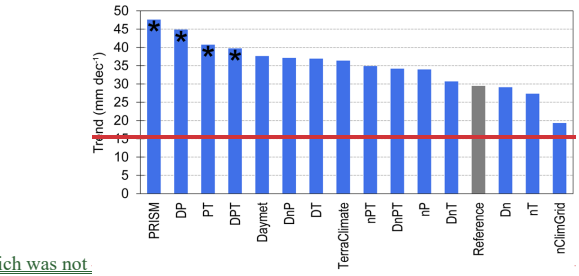

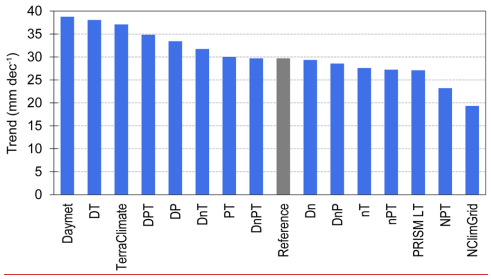

Figure 89. Precipitation increases per decade (in mm) for the reference and 15 other time series. Abbreviations for Daymet, nClimGrid, PRISM LT, and TerraClimate, are D, n, P, and T, respectively. Asterisks denote significant (α = 0.01, one-tailed) trends.

5 Discussion

5.1 Inhomogeneities and Biased Trends of Products

The introduction and proliferation of CoCoRaHS gauges—and to a lesser degree the decline of COOP gauges—caused a wetting bias in the Daymet and PRISM AN time series. Decadal precipitation increases were 28% and 62% larger, respectively, than those from the reference gauges (Fig. 6Figs. 9 and S4). CoCoRaHS gauges generally record slightly higher

precipitation totals than COOP gauges, with increases of about 1–5% (Doesken, 2005; CoCoRaHS, 2019; Goble et al., 2019). CoCoRaHS coverage in the Southeast was negligible in 2006 but reached about 75% by 2021, surpassing all other networks by 2012 and 2014 for Daymet and PRISM AN, respectively (Fig. ~~2~~4). The largest inhomogeneity in the Daymet series occurred in 2012, coinciding with this expansion. Although PRISM AN experienced similar network shifts, its main inhomogeneity appeared in 2002 due to anomalously high precipitation; correcting those values shifts the discontinuity to 2007, aligning with the network transition.

~~Expansion~~The introduction and subsequent expansion of ASOS (Automated Surface Observing Systems) gauges~~,~~ primarily deployed at airports—along with the decline of COOP gauges, produced a drying bias in nClimGrid. and, to a much lesser degree, PRISM LT. The decadal precipitation ~~increase~~increases for nClimGrid ~~was~~and PRISM LT were 34% and 9% smaller, respectively, than that of the reference series (Fig. ~~6~~9). ASOS instruments use heated tipping-bucket gauges in which each tip represents 0.01 inch of liquid-equivalent precipitation (Wade, 2003). These gauges underestimate rainfall (Dunn et al., 2025), with undercatch of 2–10% relative to COOP observations (National Research Council, 2012). ASOS coverage rose from <1% in 1993 to 19% in 2021 (Fig. ~~9~~10), while COOP coverage declined from 80% to 70% in nClimGrid and from 67% to 54% in PRISM LT (Fig. ~~2~~4). The largest inhomogeneity in nClimGrid occurred in 2005, coinciding with growing ASOS influence, whereas the largest inhomogeneity in PRISM LT occurred in 1993, coinciding with the introduction of ASOS gauges.

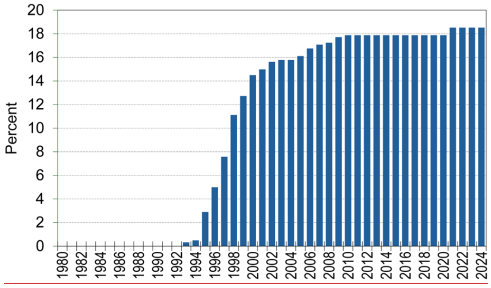

Figure 10. Percent coverage of the southeastern United States over time by Automated Surface Observing Systems (ASOS) gauges.

Formatted: Font: Not Bold

Formatted: Indent: First line: 0"

Abrupt increases in TerraClimate precipitation totals in 2011 and gridMET totals in 2016 were attributable to changes in input data. Increases in decadal precipitation for TerraClimate and gridMET were 23% and 28% larger than those of the reference gauges (~~Fig~~Figs. 6 and S5). The ~~2011~~ TerraClimate shift likely reflected ~~the substitution~~increased influence of JRA-55 anomalies following a sharp ~~gauge~~ decline in gauge observations (Abatzoglou et al., 2018~~),~~)., while the ~~2016~~ gridMET inhomogeneity coincided with a reprocessed precipitation forcing that incorporated late-reporting gauges (Xia et al., 2016~~).~~)..

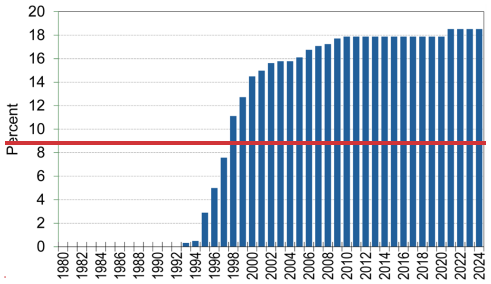

~~**Figure 9.** Percent coverage of the southeastern United States over time by Automated Surface Observing Systems (ASOS) gauges.~~

Formatted: Font: Not Bold

5.2 Optimal ~~Dataset~~Datasets for Multi-Decadal Precipitation Analyses

~~Combining Daymet and nClimGrid results in a more homogeneous and reliable dataset~~Multiple products are suitable for multi-decadal ~~precipitation~~ analyses ~~in the Southeast. Among the 15 monthly and 15 daily datasets evaluated using~~ of annual precipitation totals~~, this combination yields the fourth-smallest cumulative sum of absolute residuals (Fig. 5) and has no~~ for the southeastern United States. An optimal product should have three characteristics: (1) a relatively small cumulative residual total in the residual-mass analysis; (2) no statistically significant ~~inhomogeneities (Fig. 6). The~~ discontinuities; and (3) a precipitation trend ~~(29 mm dec^{-1}) of Daymet–nClimGrid closely matched~~ within 10% of the reference trend ~~(30 mm dec^{-1}), and no other product reproduced~~. Two product combinations—Daymet–nClimGrid and Daymet–nClimGrid–PRISM LT—meet these criteria. In these combinations, the wetting bias in Daymet is offset by the drying biases in nClimGrid and, to a lesser extent, PRISM LT. The result is a temporally stable series that exhibits no detectable discontinuities and produces a trend closely aligned with the reference ~~trend as accurately (Fig. 8). Season-specific analyses also revealed no evidence of inhomogeneities and exhibited trends nearly identical to those of the reference series (Fig. 10), further supporting the reliability of the dataset for multi-decadal assessment. Although using this dataset reduces the~~ time series. A limitation of these combined datasets is the reduction in spatial resolution ~~inherent to Daymet, the~~ resulting ~~gain in temporal homogeneity makes the~~ from use of nClimGrid, which has ~4-km grid cells that are at least 16 times larger than the ~1-km grids of Daymet ~~nClimGrid product the most robust dataset for regional, multi-~~ and PRISM LT. For applications requiring finer spatial detail, this loss of resolution may be undesirable.

PRISM LT also merits consideration as a viable individual product for multi-decadal precipitation analyses. Although the product has a statistically significant discontinuity in 1993, it produced the smallest cumulative residual total among the individual products, and its decadal ~~precipitation assessments~~trend (27 mm dec^{-1}) is within 10% of the reference trend. The 1993–2024 period can be homogenized by applying a multiplicative adjustment factor of 1.0095 derived using the mean-ratio approach outlined by Peterson et al. (1998). However, a potential long-term limitation of PRISM LT is the continued decline in COOP gauge coverage, as the product is dominated by COOP observations and further reductions in that network could decrease spatial representativeness and potentially reduce accuracy over time.

Formatted: Tab stops: 0.25", Left

6 Conclusion

Gridded precipitation datasets commonly used for hydroclimatic analyses exhibit ~~widespread~~substantial temporal inhomogeneities that can distort long-term trend assessments. Evaluation of ~~five~~six high-resolution products and their combinations for the southeastern United States during 1980–2024 revealed statistically significant ~~inhomogeneities~~discontinuities in ~~about 80% of the~~most series, ~~primarily between~~with shifts clustering in 1991–1993, 2002, 2005, 2011–2012, and ~~2018, linked to~~2016 and largely coinciding with changes in gauge networks ~~and~~or data processing. Wetting biases in Daymet and PRISM AN reflected the expansion of CoCoRaHS and decline of COOP gauges, whereas a drying bias in nClimGrid ~~arose from increased reliance on~~and, to a lesser degree, PRISM LT were associated with increasing influence of ASOS tipping-bucket gauges. ~~Step~~Abrupt step changes in TerraClimate and gridMET corresponded to documented shifts in input data and processing. These inhomogeneities produced precipitation trends ranging from 19 to 48 mm dec^{-1}, compared with a non-significant reference trend of 30 mm dec^{-1}. ~~Combining~~ Two product combinations—Daymet ~~and~~ –nClimGrid and Daymet–nClimGrid–PRISM LT—removed detectable ~~inhomogeneities~~discontinuities and ~~reproduced~~ produced trends within 10% of the reference, indicating improved temporal stability through offsetting wetting and drying biases. Despite a modest discontinuity, PRISM LT also represented a defensible standalone option because of its comparatively small cumulative residuals and near-reference trend~~, providing the most temporally stable dataset for multi-decadal analyses.~~. Overall, the ~~results~~findings underscore the ~~need to assess and, where possible, improve the~~necessity of explicitly evaluating temporal ~~stability of~~ consistency before applying gridded precipitation ~~datasets used~~products in long-term hydroclimatic analyses.

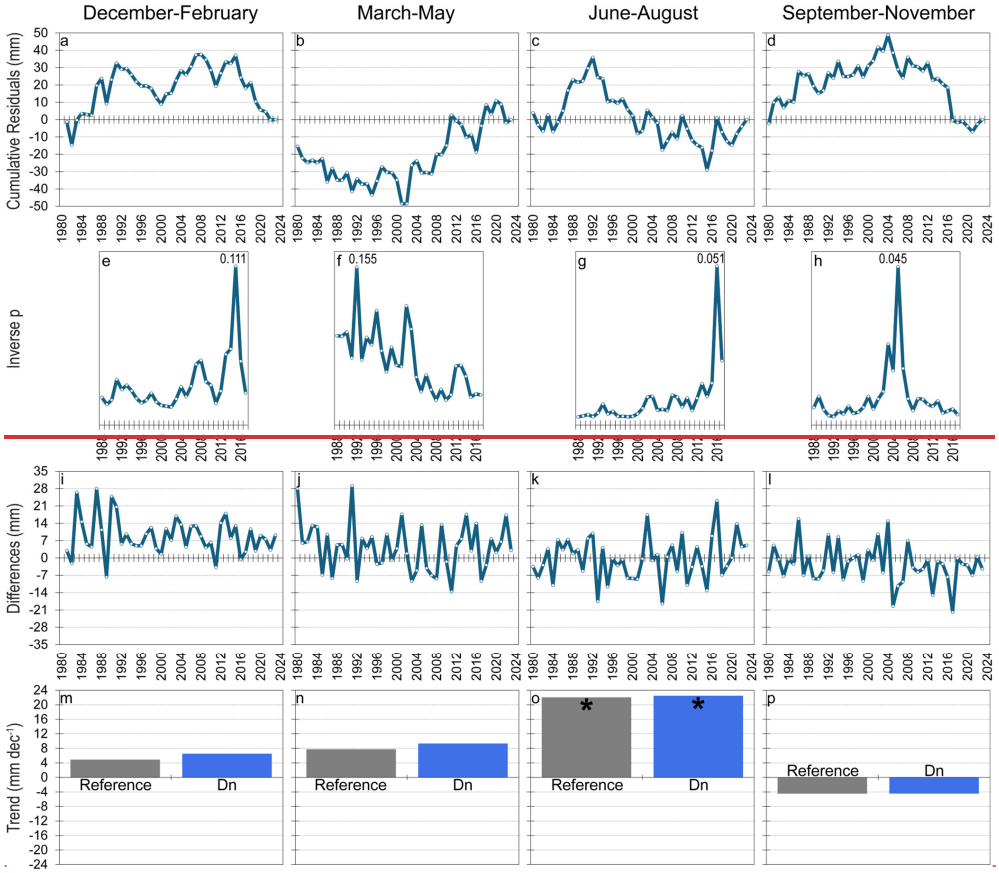

Figure 10. Residual-mass curves (a-d), inverse p-values (e-h), times series of differences (i-l), and trends (m-p) for the Daymet-nClimGrid combination for December-February, March-May, June-August, and September-November. For the inverse-p panels (e-h), the two-tailed p-values are from Mann-Whitney *U* tests that compared differences from the reference time series before and after each of the years shown (i.e., 1988-2018). The values in the difference panels (i-l) are precipitation totals from the products minus totals from the reference gauges. For the trends panels (m-p), the reference trend pertains to the reference time series and asterisks denote significant ($\alpha = 0.01$, one-tailed) trends over 1980-2023.

Data availability. Data used in this paper are available at https://data.mendeley.com/datasets/37bm8hvpmk/~~1~~2.

Competing interests. The author does not have any competing interests.

References

Abatzoglou, J. T.: Development of gridded surface meteorological data for ecological applications and modelling, Int. J. Climatol., 33, 121–131, https://doi.org/10.1002/joc.3413, 2013.

Abatzoglou, J. T., Dobrowski, S. Z., Parks, S. A., and Hegewisch, K. C.: TerraClimate, a high-resolution global dataset of monthly climate and climatic water balance from 1958–2015, Sci. Data, 5, 170191, https://doi.org/10.1038/sdata.2017.191, 2018.

Buishand, T. A.: Tests for detecting a shift in the mean of hydrological time series, J. Hydrol., 73, 51–69, https://doi.org/10.1016/0022-1694(84)90032-5, 1984.

CoCoRaHS (Community Collaborative Rain, Hail & Snow Network): Why CoCoRaHS requires manual measurements, CoCoRaHS Headquarters, Fort Collins, CO, available at: https://media.cocorahs.org/docs/Why%20CoCoRaHS%20requires%20manual%20measurements.pdf, 2019.

Daly, C., Gibson, W. P., Taylor, G. H., Doggett, M. K., and Smith, J. I.: Observer bias in daily precipitation measurements at United States Cooperative Network stations, Bull. Amer. Meteor. Soc., 88, 899–912, https://doi.org/10.1175/BAMS-88-6-899, 2007.

Daly, C., Doggett, M. K., Smith, J. I., Olson, K. V., Halbleib, M. D., Dimcovic, Z., Keon, D., Loiselle, R. A., Steinberg, B., Ryan, A. D., Pancake, C. M., and Kaspar, E. M.: Challenges in observation-based mapping of daily precipitation across the conterminous United States, J. Atmos. Ocean. Technol., 38, 1979–1992, https://doi.org/10.1175/JTECH-D-21-0054.1, 2021.

De La Fraga, P., Del-Toro-Guerrero, F. J., Vivoni, E. R., Cavazos, T., and Kretzschmar, T.: Evaluation of gridded precipitation datasets in mountainous terrains of Northwestern Mexico, J. Hydrol.: Reg. Stud., 56, 102019, https://doi.org/10.1016/j.ejrh.2024.102019, 2024.

Doesken, N.: A ten-year comparison of daily precipitation from the 4″ diameter clear plastic rain gauge versus the 8″ diameter metal standard rain gauge, Preprints, 13th Symposium on Meteorological Observations and Instrumentation, Savannah, GA, Amer. Meteor. Soc., available at: https://media.cocorahs.org/docs/AMS_NJD_GaugeComparison_AppldClimate_2-2.pdf.

Döll, P., Douville, H., Güntner, A., Müller Schmied, H., and Wada, Y.: Modelling freshwater resources at the global scale: challenges and prospects, Surv. Geophys., 37, 195–221, https://doi.org/10.1007/s10712-015-9343-1, 2016.

Durre, I., Arguez, A., Schreck, C. J., Squires, M. F., and Vose, R. S.: Daily high-resolution temperature and precipitation fields for the contiguous United States from 1951 to present, J. Atmos. Ocean. Technol., 39, 1837–1855, https://doi.org/10.1175/JTECH-D-22-0024.1, 2022.

Easterling, D. R. and Peterson, T. C.: A new method for detecting undocumented discontinuities in climatological time series, Int. J. Climatol., 15, 369–377, https://doi.org/10.1002/joc.3370150403, 1995.

Ferencz, S. B., Sun, N., Turner, S. W. D., Smith, B. A., and Rice, J. S.: Multisectoral analysis of drought impacts and management responses to the 2008–2015 record drought in the Colorado Basin, Texas, Nat. Hazards Earth Syst. Sci., 24, 1871–1896, https://doi.org/10.5194/nhess-24-1871-2024, 2024.

Ferguson, C. R. and Mocko, D. M.: Diagnosing an artificial trend in NLDAS-2 afternoon precipitation, J. Hydrometeorol., 18, 1051–1070, https://doi.org/10.1175/JHM-D-16-0251.1, 2017.

Goble, P. E., Doesken, N. J., Durre, I., Schumacher, R. S., Stewart, A., and Turner, J.: Who received the most rain today?: An analysis of daily precipitation extremes in the contiguous United States using CoCoRaHS and COOP reports, Bull. Am. Meteorol. Soc., 101, E710–E719, https://doi.org/10.1175/BAMS-D-18-0310.1, 2019.

Guentchev, G., Barsugli, J. J., and Eischeid, J.: Homogeneity of gridded precipitation datasets for the Colorado River Basin, J. Appl. Meteorol. Climatol., 49, 2404–2415, https://doi.org/10.1175/2010JAMC2484.1, 2010.

Helsel, D. R., and Hirsch, R. M.: Statistical methods in water resources, Techniques of Water-Resources Investigations, Book 4, Chapter A3, U.S. Geological Survey, available at: https://pubs.usgs.gov/twri/twri4a3/, 2002.
Henn, B., Newman, A. J., Livneh, B., Daly, C., and Lundquist, J. D.: An assessment of differences in gridded precipitation datasets in complex terrain, J. Hydrol., 556, 1205–1219, https://doi.org/10.1016/j.jhydrol.2017.03.008, 2018.
Kidd, C., Becker, A., Huffman, G. J., Muller, C. L., Joe, P., Skofronick-Jackson, G., and Kirschbaum, D. B.: So, How much of the Earth's surface is covered by rain gauges?, Bull. Am. Meteorol. Soc., 98, 69–78, https://doi.org/10.1175/BAMS-D-14-00283.1, 2017.
Kunkel, K. E., Stevens, L. E., Stevens, S. E., Sun, L., Janssen, E., Wuebbles, D., Konrad, C. E. II, Fuhrman, C. M., Keim, B. D., Kruk, M. C., Billot, A., Needham, H., Shafer, M., and Dobson, J. G.: Regional climate trends and scenarios for the U.S. National Climate Assessment. Part 2: Climate of the Southeast U.S., NOAA Tech. Rep. NESDIS 142-2, National Oceanic and Atmospheric Administration, Washington, DC, 2013.
Labosier, C. and Quiring, S.: Hydroclimatology of the Southeastern USA, Clim. Res., 57, 157–171, https://doi.org/10.3354/cr01166, 2013.
Laiti, L., Mallucci, S., Piccolroaz, S., Bellin, A., Zardi, D., Fiori, A., Nikulin, G., and Majone, B.: Testing the hydrological coherence of high-resolution gridded precipitation and temperature data sets, Water Resour. Res., 54, 1999–2016, https://doi.org/10.1002/2017WR021633, 2018.
Livneh, B., Bohn, T. J., Pierce, D. W., Munoz-Arriola, F., Nijssen, B., Vose, R., Cayan, D. R., and Brekke, L.: A spatially comprehensive, hydrometeorological data set for Mexico, the U.S., and Southern Canada 1950–2013, Sci. Data, 2, 150042, https://doi.org/10.1038/sdata.2015.42, 2015.
Mankin, K. R., Mehan, S., Green, T. R., and Barnard, D. M.: Review of gridded climate products and their use in hydrological analyses reveals overlaps, gaps, and the need for a more objective approach to selecting model forcing datasets, Hydrol. Earth Syst. Sci., 29, 85–108, https://doi.org/10.5194/hess-29-85-2025, 2025.
McAfee, S., Guentchev, G., and Eischeid, J.: Reconciling precipitation trends in Alaska: 2. Gridded data analyses, J. Geophys. Res.: Atmos., 119, https://doi.org/10.1002/2014JD022461, 2014.
Michelon, A., Benoit, L., Beria, H., Ceperley, N., and Schaefli, B.: Benefits from high-density rain gauge observations for hydrological response analysis in a small alpine catchment, Hydrol. Earth Syst. Sci., 25, 2301–2325, https://doi.org/10.5194/hess-25-2301-2021, 2021.
Mizukami, N. and Smith, M. B.: Analysis of inconsistencies in multi-year gridded quantitative precipitation estimate over complex terrain and its impact on hydrologic modeling, J. Hydrol., 428–429, 129–141, https://doi.org/10.1016/j.jhydrol.2012.01.030, 2012.
Muche, M. E., Sinnathamby, S., Parmar, R., Knightes, C. D., Johnston, J. M., Wolfe, K., Purucker, S. T., Cyterski, M. J., and Smith, D.: Comparison and evaluation of gridded precipitation datasets in a Kansas agricultural watershed using SWAT, J. Am. Water Resour. Assoc., 56, 486–506, https://doi.org/10.1111/1752-1688.12819, 2020.
National Research Council: Future of the National Weather Service Cooperative Observer Network, The National Academies Press, Washington, DC, 1998.
National Research Council: The National Weather Service modernization and associated restructuring: A retrospective assessment, The National Academies Press, Washington, DC, 2012.
New, M., Todd, M., Hulme, M., and Jones, P.: Precipitation measurements and trends in the twentieth century, Intl Journal of Climatology, 21, 1889–1922, https://doi.org/10.1002/joc.680, 2001.
Newman, A. J., Clark, M. P., Sampson, K., Wood, A., Hay, L. E., Bock, A., Viger, R. J., Blodgett, D., Brekke, L., Arnold, J. R., Hopson, T., and Duan, Q.: Development of a large-sample watershed-scale hydrometeorological data set for the contiguous USA: data set characteristics and assessment of regional variability in hydrologic model performance, Hydrol. Earth Syst. Sci., 19, 209–223, https://doi.org/10.5194/hess-19-209-2015, 2015.
Peterson, T. C., Easterling, D. R., Karl, T. R., Groisman, P., Nicholls, N., Plummer, N., Torok, S., Auer, I., Boehm, R., Gullett, D., Vincent, L., Heino, R., Tuomenvirta, H., Mestre, O., Szentimrey, T., Salinger, J., Førland, E. J., Hanssen-Bauer, I., Alexandersson, H., Jones, P., and Parker, D.: Homogeneity adjustments of in situ atmospheric climate data: a review, Int. J. Climatol., 18, 1493–1517, https://doi.org/10.1002/(SICI)1097-0088(19981115)18:13<1493::AID-JOC329>3.0.CO;2-T, 1998.
Searcy, J. K., and Hardison, C. H.: Double-mass curves, in: Manual of Hydrology: Part 1, General Surface-Water Techniques, U.S. Geological Survey Water-Supply Paper 1541-B, 31–66, 1960.

Shuai, P., Chen, X., Mital, U., Coon, E. T., and Dwivedi, D.: The effects of spatial and temporal resolution of gridded meteorological forcing on watershed hydrological responses, Hydrol. Earth Syst. Sci., 26, 2245–2276, https://doi.org/10.5194/hess-26-2245-2022, 2022.
Tang, G., Behrangi, A., Long, D., Li, C., and Hong, Y.: Accounting for spatiotemporal errors of gauges: a critical step to evaluate gridded precipitation products, J. Hydrol., 559, 294–306, https://doi.org/10.1016/j.jhydrol.2018.02.057, 2018.
Tang, G., Clark, M. P., Knoben, W. J. M., Liu, H., Gharari, S., Arnal, L., Wood, A. W., Newman, A. J., Freer, J., and Papalexiou, S. M.: Uncertainty hotspots in global hydrologic modeling: the impact of precipitation and temperature forcings, Bull. Am. Meteorol. Soc., 106, E146–E166, https://doi.org/10.1175/BAMS-D-24-0007.1, 2025.
Thornton, P. E., Shrestha, R., Thornton, M., Kao, S.-C., Wei, Y., and Wilson, B. E.: Gridded daily weather data for North America with comprehensive uncertainty quantification, Sci. Data, 8, 190, https://doi.org/10.1038/s41597-021-00973-0, 2021.
Vose, R. S., Applequist, S., Squires, M., Durre, I., Menne, M. J., Williams, C. N., Fenimore, C., Gleason, K., and Arndt, D.: Improved historical temperature and precipitation time series for U.S. climate divisions, J. Appl. Meteorol. Climatol., 53, 1232–1251, https://doi.org/10.1175/JAMC-D-13-0248.1, 2014.
Wade, C. G.: A multisensor approach to detecting drizzle on ASOS*, J. Atmos. Oceanic Technol., 20, 820–832, https://doi.org/10.1175/1520-0426(2003)020<0820:AMATDD>2.0.CO;2, 2003.
Wang, F. and Tian, D.: Hourly Evaluation of eight gridded precipitation datasets over the contiguous United States: intercomparison of satellite, radar, reanalysis, and merged products, J. Hydrometeorol., 26, 1717–1733, https://doi.org/10.1175/JHM-D-25-0063.1, 2025.
Xia, Y., Mocko, D., and Rodell, M.: An upgrade from current OPS NLDAS-2 system, in: Conference Presentation, NASA Goddard Space Flight Center, 7 July 2016.
Yang, D., Yang, Y., and Xia, J.: Hydrological cycle and water resources in a changing world: a review, Geogr. Sustain., 2, 115–122, https://doi.org/10.1016/j.geosus.2021.05.003, 2021.
Yue, S. and Wang, C. Y.: Power of the Mann-Whitney test for detecting a shift in median or mean of hydro-meteorological data, Stoch. Environ. Res. Risk Assess., 16, 307–323, https://doi.org/10.1007/s00477-002-0101-9, 2002.
Zandler, H., Haag, I., and Samimi, C.: Evaluation needs and temporal performance differences of gridded precipitation products in peripheral mountain regions, Sci. Rep., 9, 15118, https://doi.org/10.1038/s41598-019-51666-z, 2019.